Modeling of the High-Power-Factor Discontinuous Boost Rectifiers

Domingos S. L. Simonetti, *Member, IEEE,* José Luiz F. Vieira, *Member, IEEE,* and Gilberto C. D. Sousa, *Member, IEEE*

***Abstract*—This paper presents a modeling approach to obtain a small-signal model for a single-switch single-phase and three-phase discontinuous boost high-power-factor rectifiers. Such converters present nonlinear characteristics, and an approximation of them is used to derive the models. The most important result obtained is that the small-signal output impedance is not equal to the load impedance. The analysis is validated by experimental results.**

***Index Terms*—AC–DC converters, high-power-factor rectifiers, small-signal model.**

I. Introduction

ONE OF THE MOST important stages in the design procedure of a switch-mode power supply is the control loop implementation. To achieve a reliable and stable control, an adequate dynamic behavior representation is required.

Several small-, as well as large-signal, model approaches are available to determine the output voltage/control voltage transfer function and to design the compensation cell [1]–[5]. For ac–dc single-switch high-power-factor rectifiers (HPFR's) the use of a small-signal model is enough to ensure a stable operation. AC–DC rectifiers presenting unity power factor possess a well-defined linearized model around the steady-state operating point, either by using the multiplier control [6] or by using voltage-follower control [7]–[9].

Single-switch single-phase and three-phase discontinuous boost preregulators operating with constant switching frequency and duty cycle are not perfect HPFR's (the single-switch single-phase discontinuous boost HPFR is largely used as the input stage of electronic ballasts, whereas the three-phase version is a robust solution for ac–dc conversion in the 10-kVA range). The phase currents present a certain amount of low-order harmonics [10], [11]. This characteristic has an influence in the small-signal model; some of its parameters still remain nonlinear, even after small-signal approximations 12].

This paper presents a modeling approach that leads to a linearized small-signal model of the discontinuous boost HPFR. Such feature is achieved employing an approximate equation for the converter nonlinear characteristic.

Manuscript received October 30, 1997; revised December 27, 1998. Abstract published on the Internet April 18, 1999.

The authors are with the Departamento de Engenharia Elétrica, Universidade Federal do Espírito Santo, Vitória 29060-970, Brazil.

Publisher Item Identifier S 0278-0046(99)05618-X.

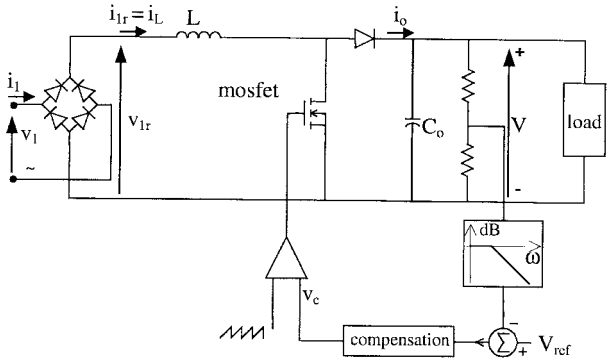

Fig. 1. A single-phase PWM-DCM boost HPFR.

II. Linearized Equation for the Nonlinear Characteristic

A. Single-Phase Discontinuous Boost HPFR

The single-switch single-phase boost topology is shown in Fig. 1. The input and output current for a few switching periods are shown in Fig. 2(a) and (b), respectively. The average input current i_1 in a switching period T_s is given by [10], [13], [14]

$$i_1 = \frac{V_1 d^2 T_s}{2L} \frac{M \sin \omega t}{(M - |\sin \omega t|)} \tag{1}$$

where V_1 is the peak ac supply voltage, d the duty cycle, L the boost inductor, ω is the line angular frequency, and the M ratio is defined by

$$M = \frac{V}{V_1} \tag{2}$$

where V is the output voltage. The input current in half of a line period (with switching harmonics filtered out) for some M ratios is shown in Fig. 2(c). To operate at discontinuous conduction mode (DCM), the converter's duty cycle must obey the inequality given by

$$d \leq \frac{M-1}{M}. \tag{3}$$

By computing the fundamental component peak value I_1 of the input current, one obtains

$$I_1 = \frac{V_1 d^2 T_s M}{2L} \frac{2}{\pi} \int_0^{\pi} \frac{\sin^2 \omega t}{M - \sin \omega t} \, d\omega t. \tag{4}$$

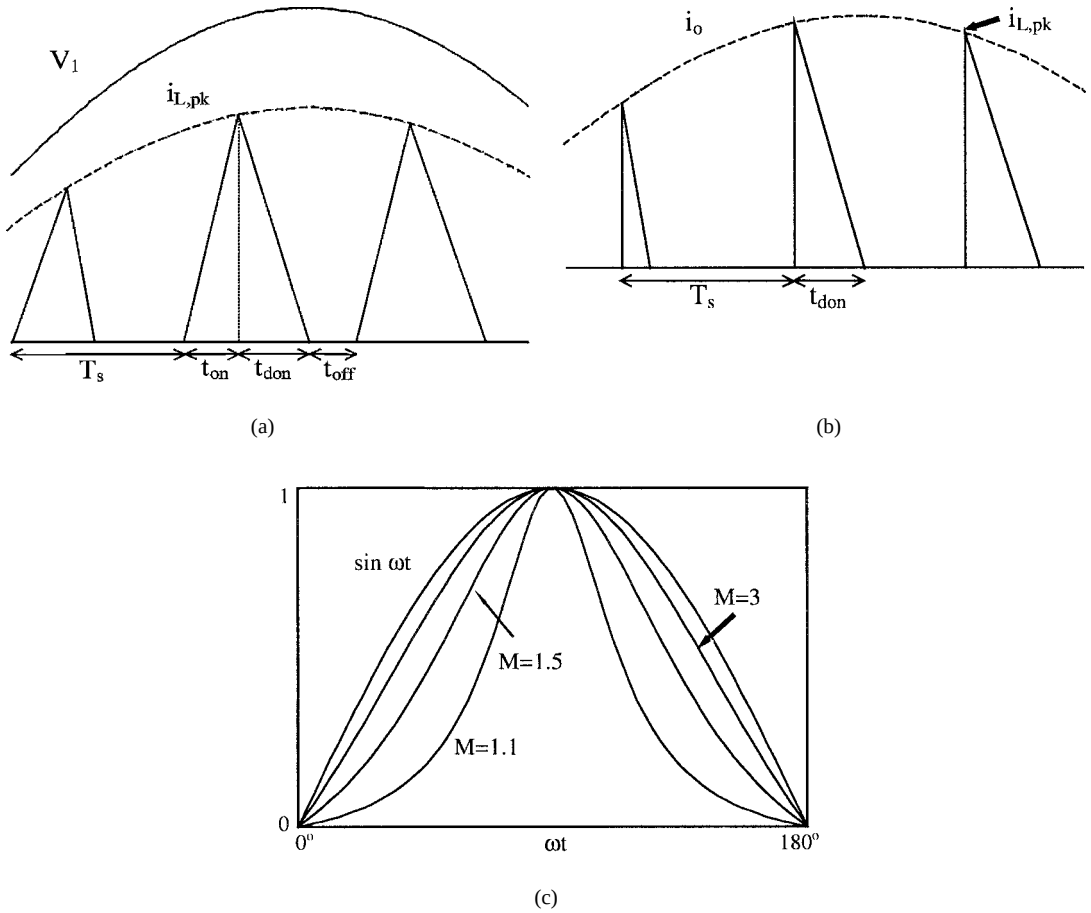

Fig. 2. (a) Input current. (b) Output current. (c) Input current with high-order harmonics filtered out.

In a similar way, the average output current i_o in a switching period is given by

$$i_o = \frac{Vd^2T_s}{2LM}\frac{\sin^2\omega t}{M-|\sin\omega t|} \tag{5}$$

while the average output current calculated over a line period (I_o) is

$$I_o = \frac{Vd^2T_s}{2LM}\frac{1}{\pi}\int_0^{\pi}\frac{\sin^2\omega t}{M-\sin\omega t}\,d\omega t. \tag{6}$$

Using (4) or (6), and the rated power of the converter $(P_{\text{rated}} = VI_o)$, the inductance L can be found

$$L = \frac{V^2d^2T_s}{2MP_{\text{rated}}}L_{\text{par}_1} \tag{7}$$

where L_{par1} is a parametric inductance given by the integral term

$$L_{\text{par}_1} = \frac{1}{\pi}\int_0^{\pi}\frac{\sin^2\omega t}{M-\sin\omega t}\,d\omega t. \tag{8}$$

L_{par1} is the nonlinear term of the single-phase DCM boost converter, and can be approximated by employing a curve-fitting software by (9) within an error less than 5% for $1.1 < M < 6$ [13]

$$L_{\text{par}_1} = \frac{0.48}{M-0.92}. \tag{9}$$

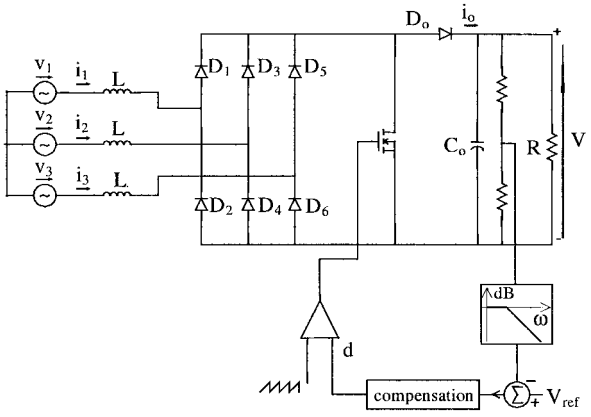

Fig. 3. Constant-frequency single-switch three-phase boost HPFR.

B. Three-Phase Discontinuous Boost HPFR

Fig. 3 shows the single-switch three-phase boost topology, whereas Fig. 4(a) and (b) shows the phase currents and the output current, respectively, for a few switching periods. Equations (10.1)–(10.4), shown at the bottom of the next page, show the computation of the average value of a phase current in a switching period over the line period [15], [16]. Fig. 4(c) shows this average current over half of a line period for some M ratios.

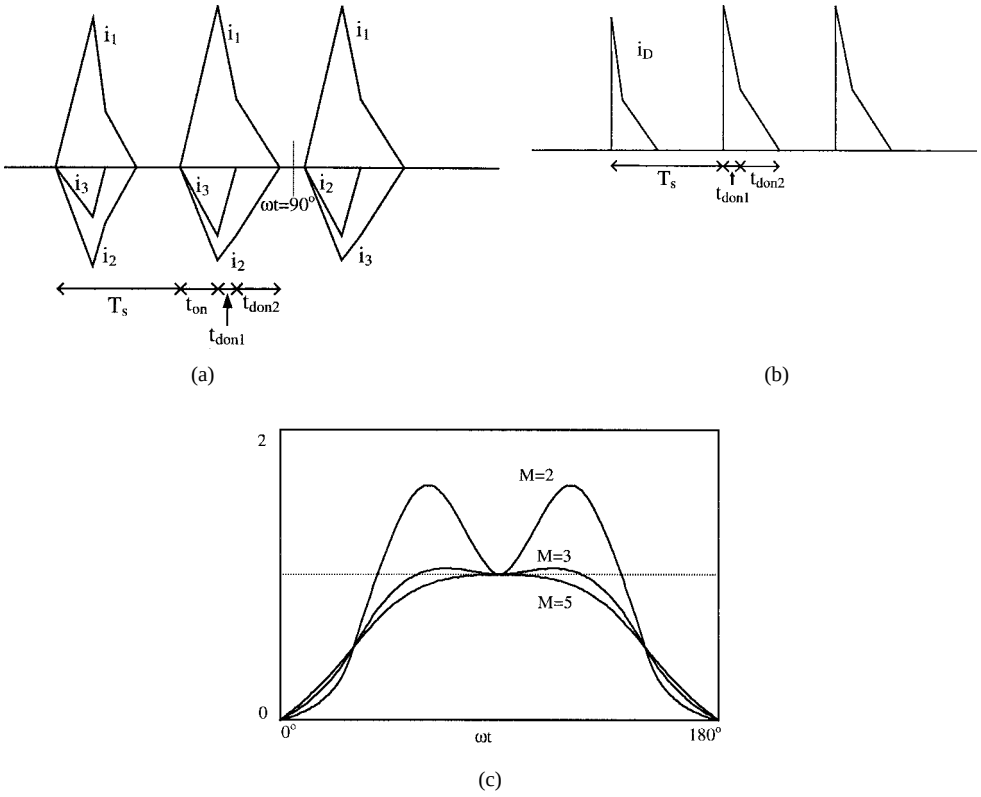

Fig. 4. (a) Inductor currents for a few switching periods. (b) Output current. (c) Shape of input current with high-order harmonics filtered out.

The single-switch three-phase boost rectifier operates at DCM if the duty cycle obeys the inequality

$$d \le \frac{M-\sqrt{3}}{M}. \tag{11}$$

The average output current over a switching period is given by (12), shown at the bottom of the page, and the average current injected into the load

$$I_o = \frac{Vd^2T_s}{2LM}L_{\mathrm{par}_3} \tag{13}$$

where

$$L_{\mathrm{par}_3} = \frac{3}{4}\frac{6}{\pi}\int_{\pi/3}^{\pi/2}\frac{2M+\sqrt{3}[\sin(3\omega t-30^\circ)-\sin(\omega t-30^\circ)]}{[M+3\sin(\omega t-240^\circ)][M-\sqrt{3}\sin(\omega t+30^\circ)]}d\omega t. \tag{14}$$

Considering $P_{\mathrm{rated}} = VI_o, L$ can be calculated as

$$L = \frac{V^2d^2T_s}{2MP_{\mathrm{rated}}}L_{\mathrm{par}_3}. \tag{15}$$

L_{par_3} is the nonlinear term of the three-phase boost converter. L_{par_3} can be approximated with good accuracy by (16)

$$i_1(\omega t) = \frac{Vd^2T_s}{2L}\frac{\sin(\omega t)}{[M-3\sin(\omega t)]}, \qquad 0^\circ \le \omega t \le 30^\circ \tag{10.1}$$

$$i_1(\omega t) = \frac{Vd^2T_s}{4L}\frac{2M\sin(\omega t)+\sqrt{3}\sin(2\omega t-120^\circ)}{[M-3\sin(\omega t-240^\circ)][M-\sqrt{3}\sin(\omega t+30^\circ)]}, \qquad 30^\circ \le \omega t \le 60^\circ \tag{10.2}$$

$$i_1(\omega t) = \frac{Vd^2T_s}{2L}\frac{M\sin(\omega t)+\sqrt{3}\sin(2\omega t+60^\circ)}{[M+3\sin(\omega t-240^\circ)][M-\sqrt{3}\sin(\omega t+30^\circ)]}, \qquad 60^\circ \le \omega t \le 90^\circ \tag{10.3}$$

$$i_1(\omega t) = i_1(180^\circ-\omega t) = -i_1(180^\circ+\omega t) = -i_1(360^\circ-\omega t) \tag{10.4}$$

$$i_o(\omega t) = \frac{3Vd^2T_s}{8ML}\left[\frac{2M+\sqrt{3}[\sin(3\omega t-30^\circ-\sin(\omega t-30^\circ)]}{[M+3\sin(\omega t-240^\circ)][M-\sqrt{3}\sin(\omega t+30^\circ)]}\right] \tag{12}$$

[17]. The error caused by the approximation is less than 5% for $1.8 < M < 6$

$$L_{\text{par}_3} = \frac{1.46}{(M - 1.67)}. \tag{16}$$

III. Small-Signal Modeling

The small-signal model is derived using the current-injected equivalent circuit approach (CIECA) [5]. In this approach, first it is necessary to find the average current injected into the converter output. Making small-signal perturbations in the average output current, the dynamic model is obtained. The perturbations used are

$$\begin{aligned} V &= \overline{V} + \hat{v} \\ V_1 &= \overline{V}_1 + \hat{v}_1 \\ I_o &= \overline{I}_o + \hat{i}_o \\ d &= \overline{D} + \hat{d} \\ I_1 &= \overline{I}_1 + \hat{i}_1 \end{aligned} \tag{17}$$

where the barred variables $(\bar{\ })$ mean the steady-state value, and the hatted variables $(\hat{\ })$ mean the perturbation introduced.

A. Single-Switch Single-Phase DCM Boost HPFR

Using (2), (6), (8), and (9), the average output current can be written as

$$I_o = \frac{V_I^2 d^2 T_s}{2L} \frac{0.48}{V - 0.92V_1} \tag{18}$$

hence,

$$I_o(V - 0.92V_1) = \frac{0.48 V_1^2 d^2 T_s}{2L}. \tag{19}$$

By substituting the small-signal perturbations given by (17) into (19), and neglecting steady-state terms, as well as perturbation products, after some algebraic manipulation [14], we obtain

$$\hat{i}_o = j_2 \hat{d} + g_2 \hat{v}_1 - \frac{1}{r_2} \hat{v} \tag{20}$$

where

$$\begin{aligned} j_2 &= \frac{0.48 \overline{DV}_1^2 T_s}{L(\overline{V} - 0.92\overline{V}_1)} \\ g_2 &= \left(\frac{0.48 \overline{V}_1 \overline{D}^2 T_s}{L} + 0.92\overline{I}_0 \right) \frac{1}{\overline{V} - 0.92\overline{V}_1} \\ r_2 &= \frac{\overline{V} - 0.92\overline{V}_1}{\overline{I}_o}. \end{aligned} \tag{21}$$

The most remarkable characteristic of the DCM single-phase boost HPFR small-signal model is that its output impedance (r_2) is not equal to the load impedance $(R_o = \overline{V}_o/\overline{I}_o)$, as usually occurs for a perfect HPFR (PF = 1) [6]. (From Fig. 2(c), it can be observed that the higher the value of M , the closer to the perfect HPFR the converter becomes.

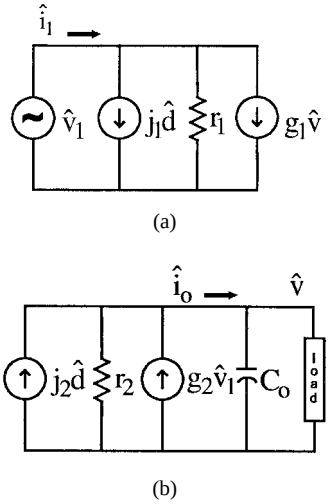

Fig. 5. Small-signal equivalent circuit. (a) Input. (b) Output.

From r_2 in (21), the higher the value of M $(V > V_1)$, the nearer r_2 is to R_o). Therefore, the equivalent output impedance r_{eq} (given by $r_{\text{eq}} = R_o r_2/(R_o + r_2)$) is not equal to $R_o/2$. In general, the time constant of the small-signal model output stage $(r_{\text{eq}} C_o)$ is smaller than that found for an ac–dc rectifier with PF = 1.

A similar analysis leads to the input-stage small-signal model. Using (2), (4), (8), and (9), we obtain

$$I_1 = \frac{V V_1 d^2 T_s}{L} \frac{0.48}{V - 0.92V_1}. \tag{22}$$

By performing small-signal perturbations and approximations, we obtain

$$\hat{i}_1 = j_1 \hat{d} + g_1 \hat{v} + \frac{I}{r_1} \hat{v}_I \tag{23}$$

where

$$\begin{aligned} j_1 &= \frac{0.96 \overline{DV}_1 \overline{V} T_s}{L(\overline{V} - 0.92\overline{V}_1)} \\ g_1 &= \left(\frac{0.48 \overline{V}_1 \overline{D}^2 T_s}{L} - \overline{I}_1 \right) \frac{1}{\overline{V} - 0.92\overline{V}_1} \\ r_1 &= -\frac{\overline{V} - 0.92\overline{V}_1}{\left(\dfrac{0.48 \overline{V} \overline{D}^2 T_s}{L} + 0.92\overline{I}_1 \right)}. \end{aligned} \tag{24}$$

The equivalent small-signal model circuit is shown in Fig. 5.

B. Single-Switch Three-Phase DCM Boost HPFR

The same approach used for the single-switch single-phase DCM boost HPFR can also be applied to the single-switch three-phase DCM boost preregulator. Using (2), (13), and (16), the average output current results in

$$I_o = \frac{V_1^2 d^2 T_s}{2L} \frac{1.46}{V - 1.67V_1} \tag{25}$$

and, by applying small-signal perturbations, an equation iden-

tical to (20) is obtained, where

$$j_2 = \frac{1.46\overline{DV}_1^2 T_s}{L(\overline{V} - 1.67\overline{V}_1)}$$
$$g_2 = \left(\frac{1.46\overline{V}_1\overline{D}^2 T_s}{L} + 1.67\overline{I}_o\right)\frac{1}{\overline{V} - 1.67\overline{V}_1}$$
$$r_2 = \frac{\overline{V} - 1.67\overline{V}_1}{\overline{I}_o}. \tag{26}$$

Once again, the remarkable characteristic of the small-signal model is that its output impedance (r_2) is not equal to the load impedance ($R_o = \overline{V}_o/\overline{I}_o$). This is an inherent characteristic of a nonideal HPFR. Considering $P_{\text{in}} = P_{\text{out}}$, the input current can be expressed as

$$I_1 = \frac{0.973VV_1 d^2 T_s}{2L(V - 1.67V_1)}. \tag{27}$$

After small-signal perturbations and approximations, an equation identical to (23) is obtained, where

$$j_1 = \frac{0.973\overline{DV}_1\overline{V}T_s}{L(\overline{V} - 1.67\overline{V}_1)}$$
$$g_1 = \left(\frac{0.487\overline{V}_1\overline{D}^2 T_s}{L} - \overline{I}_1\right)\frac{1}{\overline{V} - 1.67\overline{V}_1}$$
$$r_1 = \frac{\overline{V} - 1.67\overline{V}_1}{\left(\dfrac{0.487\overline{VD}^2 T_s}{L} + 1.67\overline{I}_1\right)}. \tag{28}$$

The small-signal equivalent circuit is the same one shown in Fig. 5.

IV. Experimental Results

A single-phase and a three-phase prototype were built to verify the actual small-signal behavior of a single-switch DCM boost HPFR and to compare with the developed model.

A. Single-Phase Implementation

A single-phase converter feeding a resistive load was built with the following data:

input voltage	$V_{1,\text{rms}} = 120\,\text{V}, 60\,\text{Hz}$ $(V_1 = 170\,\text{V})$;
output voltage	$V = 380$ V (dc);
switching frequency	$f_s = 40$ kHz;
output resistance	$R_o = 1600\,\Omega$ $(P_{\text{rated}} = 90$ W);
output capacitor	$C_o = 235\,\mu$F;
inductance	$L = 227\,\mu$H;
steady-state duty cycle	$d = 0.245$.

The input voltage and current for rated load are shown in Fig. 6, where the power factor is close to 0.99. Substituting the values given above into (21) yields

$$j_2 = 1.67 \quad g_2 = 0.0034 \quad r_2 = 942\,\Omega. \tag{29}$$

Observe that the small-signal impedance is about 60% of R_o (and not equal to it). The equivalent output impedance

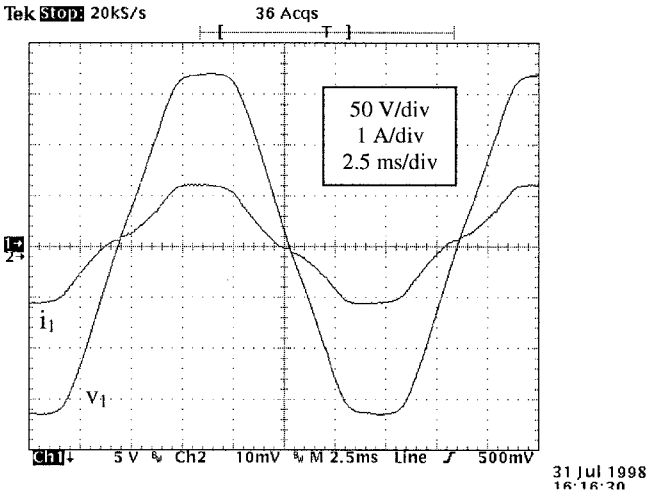

Fig. 6. Input voltage and current of the single-phase boost HPFR.

is $r_{\text{eq}} = 593\,\Omega$. From the small-signal equivalent circuit, the following transfer functions are obtained:

$$\frac{\hat{v}}{\hat{d}} = \frac{j_2 r_{\text{eq}}}{r_{\text{eq}}C_o s + 1} = \frac{990.3}{0.14s + 1}$$
$$\frac{\hat{v}}{\hat{v}_1} = \frac{g_2 r_{\text{eq}}}{r_{\text{eq}}C_o s + 1} = \frac{20.2}{0.14s + 1}. \tag{30}$$

Small-signal perturbations around the operating point are applied to observe its small-signal open-loop response. First, the duty-cycle was submitted to a step change from 0.245 to 0.215 ($\hat{d} = -0.03$). Using (30), the expected small-signal output response is

$$\hat{v}(t) = -30(1 - e^{-(t/0.14)}) \quad \text{V}. \tag{31}$$

The settling time is about 560 ms. Fig. 7(a) shows the result obtained for the prototype. The actual small-signal open-loop response can be written as

$$\hat{v}(t) = -33(1 - e^{-t/0.135}) \quad \text{V}. \tag{32}$$

As can be seen, the experimental result is close to the expected one. A similar test was realized using $\hat{d} = 0.032$. The theoretical small-signal response is

$$\hat{v}(t) = 32(1 - e^{-(t/0.14)}) \quad \text{V}. \tag{33}$$

The actual response is shown in Fig. 7(b), and can be represented by

$$\hat{v}(t) = 35(1 - e^{-t/0.135}) \quad \text{V}. \tag{34}$$

Next, a step change was applied to the input voltage ($\hat{v}_1 = 24\,\text{V} \Rightarrow V_{1,\text{rms}}$ change from 120 to 137 V). The theoretical result using (30) is

$$\hat{v}(t) = 48(1 - e^{-(t/0.14)})\,\text{V}. \tag{35}$$

The actual response is shown in Fig. 7(c). It can be described by

$$\hat{v}(t) = 50(1 - e^{-t/0.135})\,\text{V}. \tag{36}$$

As have occurred for (31) and (32), (33) and (34), as well as (35) and (36), are very close. These results show that the

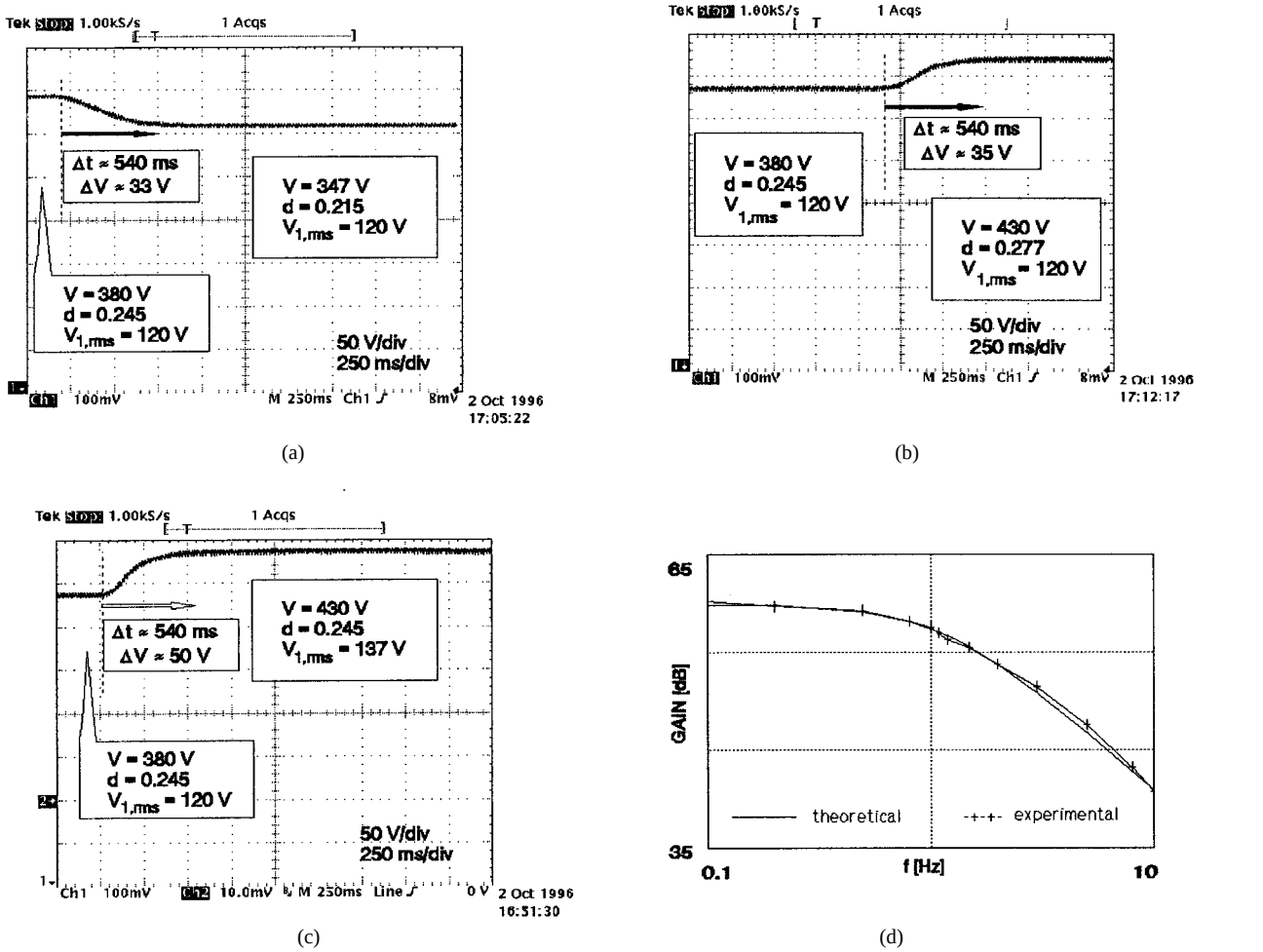

Fig. 7. Open-loop output voltage response, single-phase HPFR, $R_o = 1600\,\Omega$. (a) A small step reduction in the duty cycle. (b) A small step increase in the duty cycle. (c) A small step increase in the input voltage. (d) Experimental and theoretical $\hat{v}/\hat{d}$ Bode diagram.

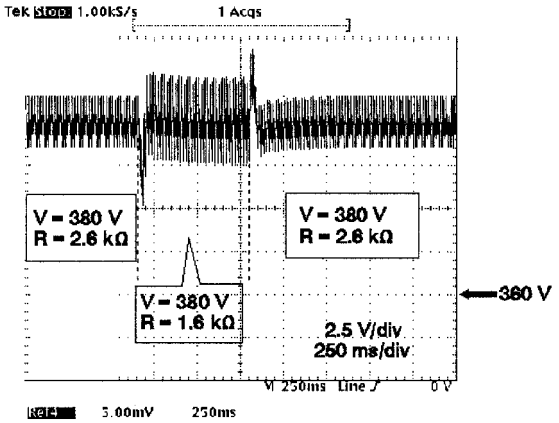

Fig. 8. Closed-loop output voltage response to a load step variation, single-phase boost HPFR.

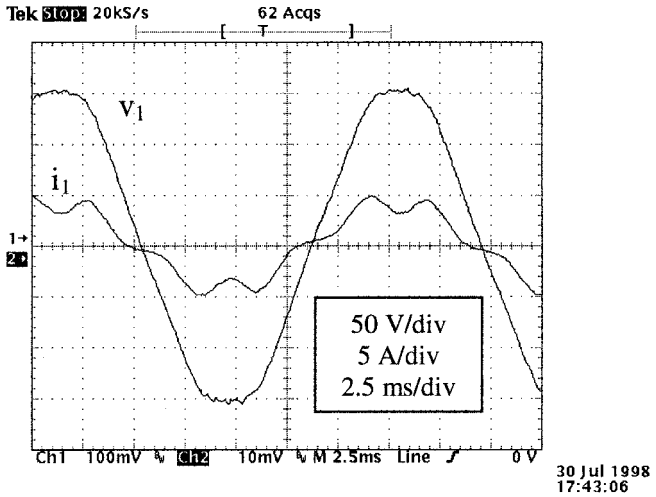

Fig. 9. Input voltage and current of the three-phase boost HPFR.

model obtained here represents with good precision the actual small-signal behavior of the converter. The experimental $\hat{v}/\hat{d}$ transfer function Bode diagram, as well as the theoretical one, are shown in Fig. 7(d), and one can see that the developed model is very accurate. Fig. 8 shows a closed-loop response of such converter, where the compensation loop was designed considering the transfer function developed here. Initially, the converter was supplying 55 W to the load. At $t = t_1$, the load is suddenly increased to 90 W, while at $t = t_2$, it is reduced back to 55 W. It can be noticed that a very small voltage fluctuation occurs and that the loop response is adequate.

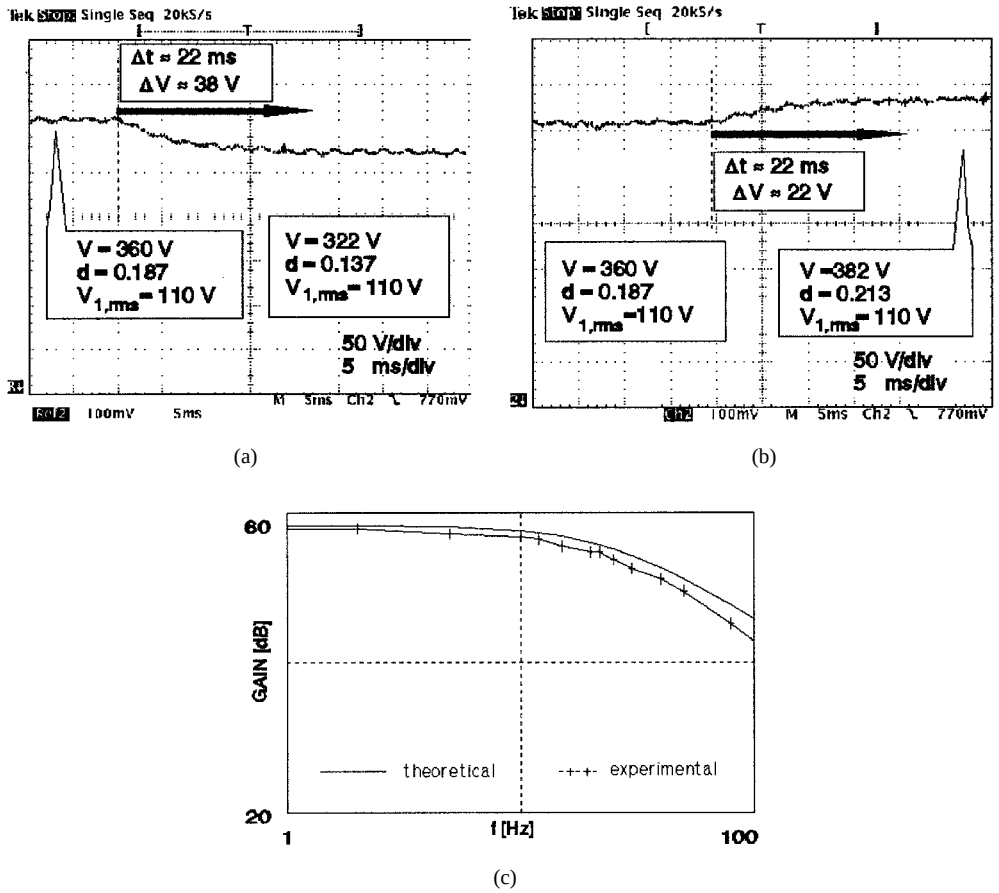

(a) (b) (c)

Fig. 10. (a) Open-loop output voltage response, three-phase HPFR, $R_o = 130\,\Omega$. (a) For a small step reduction in the duty cycle. (b) For a small step increase in the duty-cycle. (c) Experimental and theoretical $\hat{v}/\hat{d}$ Bode diagram.

B. Three-Phase Implementation

A single-switch three-phase boost HPFR was built with the following characteristics:

input voltage	$V_{1,\mathrm{rms}} = 110$ V, 60Hz $(V_1 = 156$ V);
output voltage	$V = 360$ V (dc);
switching frequency	$f_s = 40$ kHz;
output resistance	$R_o = 130\,\Omega$ ($P_{\mathrm{rated}} = 1$ kW);
output capacitor	$C_o = 220\,\mu$F;
inductance	$L = 61\,\mu$H;
steady-state duty cycle	$d = 0.187$.

The input voltage and current for rated load are shown in Fig. 9, where the power factor is close to 0.98. Using the values given above into (26) yields

$$j_2 = 28 \quad g_2 = 0.08 \quad r_2 = 37\,\Omega \tag{37}$$

and the transfer functions

$$\frac{\hat{v}}{\hat{d}} = \frac{812}{0.0064s + 1}$$
$$\frac{\hat{v}}{\hat{v}_1} = \frac{2.32}{0.0064s + 1}. \tag{38}$$

Here, small-signal perturbations were also introduced to observe the small-signal response. For a duty-cycle step change of $\hat{d} = -0.05$, and from (38), the theoretical response is

$$\hat{v}(t) = -41(1 - e^{-(t/0.0064)})\ \mathrm{V}. \tag{39}$$

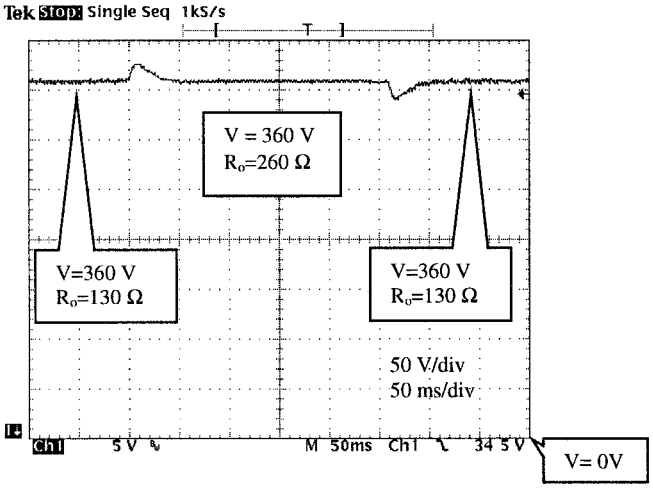

Fig. 11. Closed-loop output voltage response to a load step variation, three-phase boost HPFR.

The settling time is about 25.5 ms. Fig. 10(a) shows the actual response, that can be written as

$$\hat{v}(t) = -38(1 - e^{-(t/0.0055)})\ \mathrm{V}. \tag{40}$$

On the other hand, by applying a duty-cycle step change of $\hat{d} = 0.026$, from (38) the theoretical response can be obtained

as

$$\hat{v}(t) = 21(1 - e^{-(t/0.006)}) \text{ V}. \quad (41)$$

The experimental result is shown in Fig. 10(b) and can be described by

$$\hat{v}(t) = 22(1 - e^{-(t/0.0055)}) \text{ V}. \quad (42)$$

The theoretical results given by (39) and (41) are close to the actual responses given by (40) and (42), respectively. Fig. 10(c) shows the theoretical and experimental $\hat{v}/\hat{d}$ converter transfer function Bode diagrams, which are very similar. These facts show the adequacy of the developed model.

Fig. 11 shows a closed-loop response of the implemented converter. The load is changed from its rated value (1 kW) to half of it (500 W) and then returned to the rated value. Good dynamic response is obtained.

V. Conclusions

Small-signal models for single-switch single- and-three-phase boost HPFR's were presented here. Such models were developed from a linearization of nonlinear terms present in some of the descriptive equations of the converters. Both input and output small-signal models are easily derived. The most relevant characteristic of the small-signal models of such converters is that the small-signal output impedance r_2 is not equal to R_o, but always smaller than it. Experimental open-loop results and Bode diagrams were compared to theoretical ones and found to closely agree with one another, which confirms the validity of the models.

Acknowledgment

The authors thank E. Pascual and M. C. Azevedo for their help in building the single-phase and three-phase prototypes, respectively.

References

[1] R. D. Middlebrook and S. Cuk, "A general unified approach to modeling switching converters power stage," in *Proc. IEEE PESC'76*, 1976, pp. 18–34.
[2] R. W. Erickson, S. Cuk, and R. D. Middlebrook, "Large-signal modeling and analysis of switching regulators," in *Proc. IEEE PESC'82*, 1982, pp. 240–250.
[3] C. K. Tse and K. M. Adams, "Quasilinear modeling and control of DC-DC converters," *IEEE Trans. Power Electron.*, vol. 7, pp. 315–323, Apr. 1992.
[4] M. Rico, V. Garcia, M. Hernando, F. Nuño, J. Sebastián, and J. Uceda, "A unified method to model resonant switching converters," in *Proc. IEEE IECON'90*, 1990, pp. 964–969.
[5] P. R. K. Chetty, "Current injected equivalent circuit approach (CIECA) to modeling of switching dc-dc converters," *IEEE Trans. Aerosp. Electron. Syst.*, vol. 17, pp. 802–808, Nov. 1981.
[6] R. B. Ridley, "Average small-signal analysis of the boost power factor correction circuit," in *Proc. VPEC Seminar*, 1989, pp. 108–120.
[7] R. Erickson, M. Madigan, and S. Singer, "Design of a simple high-power-factor rectifier based on the flyback converter," in *Proc. IEEE APEC'90*, 1990, pp. 792–801.
[8] D. Simonetti, J. Sebastián, and J. Uceda, "A small-signal model for sepic, Cuk, and flyback converters as power factor prerregulators in discontinuous conduction mode," in *Proc. IEEE PESC'93*, 1993, pp. 735–741.
[9] ——, "A novel three-phase AC-DC power factor preregulator," in *Proc. IEEE PESC'95*, 1995, pp. 979–984.
[10] K. H. Liu and Y. L. Lin, "Current waveform distortion in power factor correction circuits employing discontinuous mode boost converter," in *Proc. IEEE PESC'89*, 1989, pp. 825–829.
[11] E. Ismail and R. Erickson, "A single transistor three phase resonant switch for high quality rectification," in *Proc. IEEE PESC'92*, 1992, pp. 1341–1351.
[12] T. C. Chen and C. T. Pan, "Modeling and design of a single phase AC to DC convertor," *Proc. Inst. Elect. Eng.*, vol. 139, pt. B, no. 5, pp. 465–470, Sept. 1992.
[13] D. Simonetti, J. L. F. Vieira, J. Sebastián, and J. Uceda, "Simplifying the design of a DCM boost PFP," in *Proc. IEEE CIEP'96*, 1996, pp. 138–141.
[14] D. Simonetti, "AC-DC preregulators with power factor correction. Single-switch solutions," Ph.D. dissertation, Dep. Electron. Eng., Univ. Politécnica de Madrid, Madrid, Spain, Nov. 1995.
[15] D. Simonetti, J. Sebastián, and J. Uceda, "Single-switch three-phase power factor preregulator under variable switching frequency and discontinuous input current," in *Proc. IEEE PESC'93*, 1993, pp. 657–662.
[16] J. W. Kolar, H. Ertl, and F. C. Zach, "Space vector-based analytical analysis of the input current distortion of a three-phase discontinuous-mode boost rectifier system," in *Proc. IEEE PESC'93*, 1993, pp. 696–703.
[17] D. Simonetti, J. Sebastián, and J. Uceda, "A simplified design approach for constant-frequency single-switch three-phase discontinuous boost power factor preregulators," in *Proc. IEEE ISIE'97*, 1997, pp. 578–582.

Domingos S. L. Simonetti (S'92–M'95 received the degree in electrical engineering from the Federal University of Espírito Santo, Vitória, Brazil, the M.S. degree from the Federal University of Santa Catarina, Florianópolis, Santa Catarina, Brazil, and the Ph.D. degree from the Polytechnical University of Madrid, Madrid, Spain, in 1984, 1987, and 1995, respectively.

Since 1984, he has been a Professor in the Electrical Engineering Department, Federal University of Espírito Santo. His research interests include high-power-factor rectifiers, active power filters, low-loss converters, and machine drives.

José Luiz F. Vieira (S'90–M'95) received the degree in electrical engineering from the Federal University of Espírito Santo, Vitória, Brazil, the M.S. degree from COPPE/Federal University of Rio de Janeiro, Rio de Janeiro, Brazil, and the Ph.D. degree from the Federal University of Santa Catarina, Florianópolis, Brazil, in 1981, 1986, and 1993, respectively.

Since 1982, he has been a Professor in the Electrical Engineering Department, Federal University of Espírito Santo. His research interests include high-efficiency and high-power-factor converters and electronic illumination systems.

Prof. Vieira is a member of the Brazilian Power Electronics Society (SOBRAEP) and Brazilian Society of Automatic Control (SBA).

Gilberto C. D. Sousa (S'91–M'93) received the B.Sc. degree from the Federal University of Espírito Santo, Vitória, Brazil, the M.Sc. degree from the Federal University of Santa Catarina, Florianópolis, Brazil, and the Ph.D. degree from the University of Tennessee, Knoxville, all in electrical engineering.

He has been with the Electrical Engineering Department, Federal University of Espírito Santo, since 1982, where he has been teaching power systems and electrical machines and drives courses to graduate and undergraduate students. His research interests includes high-performance drives, power-factor correction, and emerging technologies.

Dr. Souza is a member of the IEEE Industry Applications Society, Brazilian Society of Automatic Control, and Brazilian Power Electronics Society.